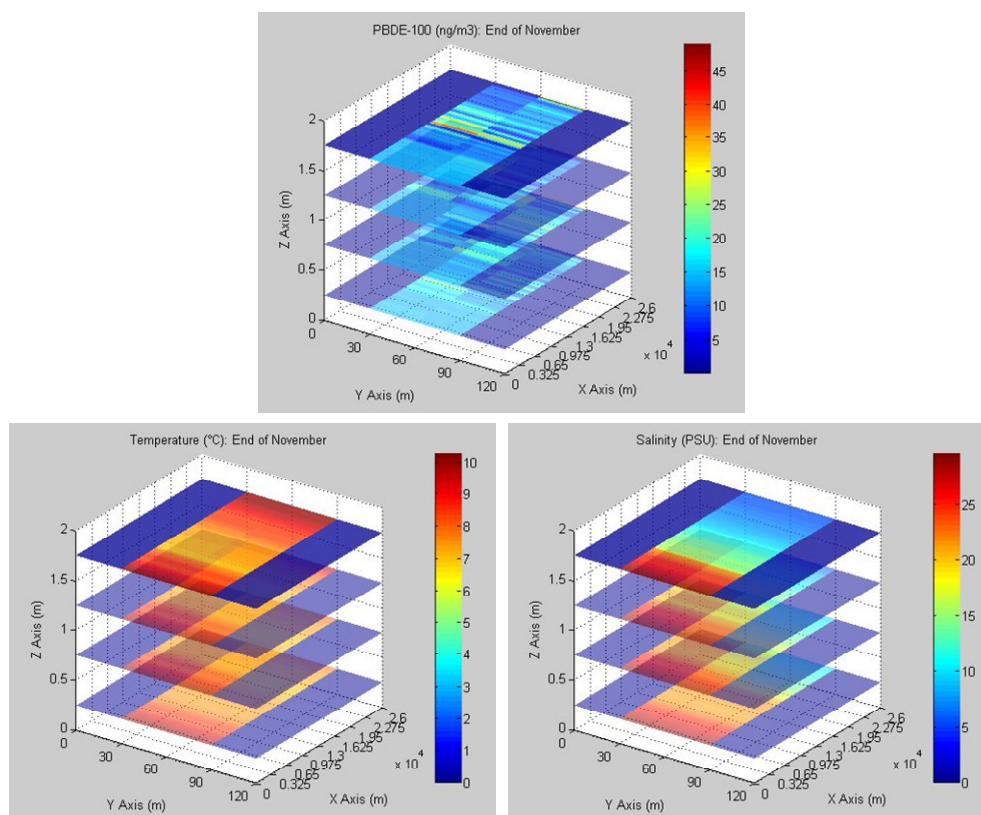


Polybrominated Diphenyl Ethers (PBDEs) fate and transport in an estuary using a three-dimensional hydrodynamic modelling approach

R.O. Strobl, I. Puillat, D. Marinov, S. Dueri and J. M. Zaldívar



EUR 23227 EN - 2007

The mission of the Institute for Environment and Sustainability is to provide scientific-technical support to the European Union's Policies for the protection and sustainable development of the European and global environment.

European Commission
Joint Research Centre

Contact information

Address: Via E. Fermi 1, TP 272
E-mail: jose.zaldivar-comenges@jrc.it
Tel.: +39-0332-789202
Fax: +39-0332-785807

<http://www.jrc.ec.europa.eu>

Legal Notice

Neither the European Commission nor any person acting on behalf of the Commission is responsible for the use which might be made of this publication.

A great deal of additional information on the European Union is available on the Internet. It can be accessed through the Europa server
<http://europa.eu/>

JRC 42292

EUR 23227 EN

ISSN 1018-5593

Luxembourg: Office for Official Publications of the European Communities

© European Communities, 2007

Reproduction is authorised provided the source is acknowledged

Printed in Italy

Table of Contents

1. INTRODUCTION	5
1.1. PAST ESTUARY MODELLING STUDIES	7
1.2. POLYBROMINATED DIPHENYL ETHERS (PBDEs)	9
1.3. OBJECTIVES	10
2. MODEL DESCRIPTION.....	10
2.1. HYDRODYNAMIC MODULE	10
2.2. CONTAMINANT FATE MODULE.....	13
3. EXEMPLARY CASE STUDIES.....	14
4. RESULTS AND DISCUSSION.....	17
4.1. 3-DAY SIMULATION	17
4.2. 1-YEAR SIMULATION.....	21
5. CONCLUSIONS.....	23
6. REFERENCES	25

List of Tables

Table 3.1: Typical PBDE-100 ranges and corresponding references.....	16
--	----

List of Figures

Figure 1.1. Estuary types defined by amount of mixing between freshwater (0 ‰) and seawater (34 ‰) (Garrison, 1995)	7
Figure 2.1. Schematic view of the hydrodynamic module of the COHERENS model	11
Figure 2.2. Overview of the processes included in the contaminant fate module	14
Figure 3.1. Case study schematic	15
Figure 3.2. Tidal depth for the period 01/01/2003 – 03/01/2003	17
Figure 3.3. Theoretically measured temperature and salinity distribution at the open sea and river ends for the simulation period	17
Figure 4.1. Temperature distribution for Day 1 at 08h00, Day 1 at 16h00 and Day 2 at 08h00	18
Figure 4.2. Salinity distribution for Day 1 at 08h00, Day 1 at 16h00 and Day 2 at 08h00	18
Figure 4.3. PBDE-100 distribution for Day 1 at 08h00, Day 1 at 16h00 and Day 2 at 08h00	19
Figure 4.4. Temperature distribution for Day 2 at 17h00, Day 2 at 09h00 and Day 3 at 17h00	19
Figure 4.5. Salinity distribution for Day 2 at 17h00, Day 2 at 09h00 and Day 3 at 17h00	19
Figure 4.6 PBDE-100 distribution for Day 2 at 17h00, Day 2 at 09h00 and Day 3 at 17h00	19
Figure 4.7. Point locations of observed temporal evolutions	20
Figure 4.8. Temperature, Salinity and PBDE-100 concentration during the 3-day simulation period (Point A: sea side)	21
Figure 4.9. Temperature, Salinity and PBDE-100 concentration during the 3-day simulation period (Point B: centre channel)	21
Figure 4.10. Temperature, Salinity and PBDE-100 concentration during the 3-day simulation period (Point A: river side)	21
Figure 4.11. Temperature, salinity and PBDE-100 concentration at sea side (2003)	22
Figure 4.12. Temperature, salinity and PBDE-100 concentration at centre channel (2003)	23
Figure 4.13. Temperature, salinity and PBDE-100 concentration at river side (2003)	23

1. INTRODUCTION

By definition, a water mass is a large body of water having a unique set of properties, typically identified by its salinity and temperature (OSPAR, 2000). In fact, the salinity and temperature are the principal factors that determine the water density. Depending on its density, an incoming water mass mixing with a given water body will sink or rise to a given equilibrium depth. Mixing in the vertical plane may take place due to wind, tidal movements or currents, and can produce thermally stratified waters (Wunsch and Ferrari, 2004).

One such water body that is affected by the salinity and temperature distributions is an estuary. An estuary is a saltwater-freshwater interface ecosystem and represents the section of the lower river course where its current encounters incoming coastal tides. As a consequence, salinity levels are typically lowest upstream where freshwater enters and highest in the vicinity of the mouth of a river where seawater flows in. The salinity-reducing effects of freshwater inflow into an estuary are most discernible after heavy rainfall periods. Nevertheless, the salinity level at a specific location within the estuary fluctuates according to the tidal cycle. As a result, this continuous mixing of fresh- and seawater generates a productive environment that provides animal and plant habitats. The result of such transitional areas is brackish waters that are able to support a high level of biodiversity. Salinity plays a major role in the dynamics of an estuary as it also affects its chemical conditions, especially dissolved oxygen levels. In general, an increase in salinity decreases the amount of dissolved oxygen, or solubility (U.S. EPA, 2006). These variations in salinity levels ultimately result in changes in species abundance, composition and distribution in an estuary. As a consequence, most species live under stress in an estuary, either due to elevated or decreased salinity levels, depending if their origin is marine or freshwater (Kautsky, 1998). Furthermore, nutrients originating from the sea, land and inflowing river systems are washed out and then trapped within an estuary. Through tidal movement, currents and wind, these nutrients as well as organic matter and toxic substances are dispersed throughout the estuary ecosystem. Often these inflows consist of large amounts of inorganic as well as organic matter which can raise turbidity levels and consequently reduce the primary production by benthic macroalgae and rooted aquatic plants. Nonetheless, many aquatic plants are able to survive exposed to below optimal light levels for extended periods (Batiuk et al., 2000). On the other hand, the reduction of nutrient loads, such as by improving the performance of upstream wastewater treatment plants, can enhance light conditions. These improved conditions can permit the growth of macrophytes on sediment bottoms which in turn will be able to demobilize, for example, heavy metals deposited deeply in the sediment (Greger et al., 1995). In addition,

salinity controls sedimentation and flocculation mechanisms in estuaries, changing the availability of metals. As a general rule, the total concentration of heavy metals in seawater is much lower than in freshwater (Kautsky, 1998). With a salinity gradient present, generally the speciation of heavy metals will change in the water towards heavy metal complexes in saltwater that are less bioavailable compared to the heavy metals in freshwater.

Similarly to nutrients, other chemical constituents are dispersed throughout the system due to these movements. Depending on the contaminant in question, its concentration can decrease or increase with increasing salinity. Similarly to metals, POPs (Persistent Organic Pollutants) will be affected by the salinity gradient in estuaries. In a series of recent studies (Turner and Rawling, 2001; Turner, 2003) observed that the change (decrease) of solubility of chemicals (salting out) was not sufficient to account for the changes observed in estuaries and suggested that the hydrophobicity of sediment organic matter is also modified by interactions with dissolved sea water ions. In addition, the buoyancy effects in estuaries due to salinity and temperature play a major role and are driven through the often rapid changes in the distributions of salinity and temperature (Jackson and Rehmann, 2003). These changes in salinity and temperature also affect the persistence, survival as well as emergence of various species in estuaries. In addition, temperature affects all biogeochemical reactions in an aquatic system, including microbial activity. Therefore, it is quite important to incorporate the spatial and temporal evolution of the temperature and salinity distributions in any hydrodynamic model aiming at accurately representing an estuary ecosystem. The salinity profile is often used to distinguish different types of estuaries, as shown in Fig. 1.1 (Garrison, 1995). As demonstrated in Fig. 1.1, the salinity structure in an estuary is a result of the interplay between the buoyancy flux from the freshwater inflow, advection by tides and circulation, as well as mixing.

In recent years, the European Union has invested a substantial amount of financial resources into the development of a knowledge base for the identification and better understanding of the key factors that affect coastal waters and their interaction with corresponding watersheds. In addition, this effort has strived to better understand the impact of different land uses on contaminant loads ultimately reaching coastal zones. In particular, estuarial ecosystems are exposed to anthropogenic threats related to their use as well as to the impact of polluting sources draining into and through them (UNEP, 2004). As a result, estuaries exhibit a host of environmental problems, including the following factors:

- destruction of wetlands part of the estuarial ecosystem
- habitat alteration and degradation
- incoming contaminants
- urban and industrial expansion

- logging and fishing activities
- impact of dredging
- marine transportation impact

From an ecological, social as well as economic point of view, estuaries are valuable resources in several ways including as (UNEP, 2004):

- contaminant traps
- plant and wildlife habitat, including spawning, nursery and feeding grounds
- food source for wildlife
- detoxification of wastes
- nutrient cycling
- buffers for flooding
- shoreline and stream bank stabilisation from erosion
- water supply for municipalities, agriculture and industry
- recreation and tourism
- commercial and sport fisheries

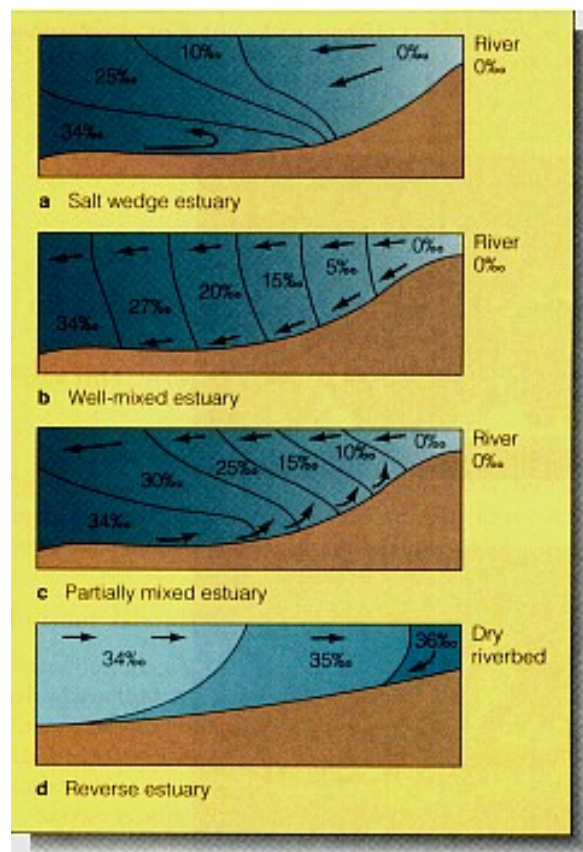


Figure 1.1 – Estuary types defined by amount of mixing between freshwater (0 ‰) and seawater (34 ‰) (Garrison, 1995).

1.1 Past estuary modelling studies

In recent years there have been a number of estuarine modelling attempts (e.g. Nunes Vaz et al., 1989; Simpson et al., 1990; Simpson et al., 1991; Simpson and Sharples, 1991; Nunes Vaz and Simpson, 1994; Monismith and Fong, 1996; Zhou, 1998) with one-dimensional (i.e.,

vertical) representations of the salinity and velocity fields. These studies have examined the interactions between tidal mixing, stratification and shear, as well as assessed turbulence closure models. Tidal stratification in estuaries is a complex transient mechanism that is influenced by the forces of vertical gravitational circulation and longitudinal density gradient by vertical shear in competition with the mixing influence of tidally generated turbulence (Liu et al. 2002). Turbulence closure models, on the other hand, are used extensively in ocean hydrodynamic studies, particularly in the investigation of mixing and stratification and their effect on ocean biological processes (Wei et al., 2001). Nonetheless, Warner et al. (2005) reports that one-dimensional models often disagree considerably when confronted with in-field observations. Inadequate turbulence closure or unresolved variations of the salinity gradient may be partially to blame for these discrepancies (Simpson and Sharples, 1991).

As has been established by Chatwin (1976) as well as by Hansen and Rattray (1965) in classical estuarine theory, the longitudinal salinity gradient is in fact not an independent variable, but instead part of the solution of the salinity and momentum conservation equations for a particular freshwater outflow. While the solution by Chatwin (1976) imposes that the salinity gradient varies vertically so as to satisfy the overall salinity balance, the solution by Hansen and Rattray (1965) makes the assumption of zero vertical variation in salinity gradient. Nevertheless, there is a large temporal variability of the longitudinal salinity gradient, mainly due to variations caused by runoff inputs (Kranenburg, 1986). In addition, there are variations of the salinity gradient with tidal amplitude, as demonstrated by numerical models applied by MacCready (1999) and Hetland and Geyer (2004). Thus, these previous investigations have shown that the salinity gradient should be incorporated as a dependent variable. This, on the other hand, implies that one-dimensional models are generally limited as prognostic tools.

Contrary, three-dimensional estuarine models include the longitudinal salinity gradient as a dependent variable. The few three-dimensional estuarine applications that have been undertaken and reported in the literature, have investigated the variability of the longitudinal salinity gradient in addition to the variability of the stratification, and tidal and mean shear. These studies have shown limited agreement between simulation and observation results in terms of the sensitivity of saltwater intrusion to tidal range and river flow (Prandle, 2004). In a study comparing different turbulence closure models, Li et al. (2005) have observed that model performance was weak in the stratified pycnocline region, but acceptable for the mixing in the bottom boundary layer. Model results by Stenstrom (2004) of a simulation for a neap semidiurnal tidal cycle in the Hudson River estuary, on the other hand, compared fairly

well with a limited observation set. Nevertheless, Stenstom (2004) concluded that further studies and more rigorous model testing are required to improve the turbulence closure schemes. Also, North et al (2004) have concluded that in order to improve and realistically model estuarine circulation it is necessary to develop better parameterizations of turbulence in stratified flows. In summary, these studies have shown that the inconsistencies between simulation results and observed data were principally due to the application of inadequate forcing data, unsatisfactory grid resolution or inadequate turbulence closure schemes.

1.2 Polybrominated diphenyl ethers (PBDEs)

POPs (Persistent Organic Pollutants) are a set of toxic organic chemicals that are persistent in the environment for long periods of time. In general, they are susceptible to bioaccumulation and biomagnification through the food chain. Since they circulate globally both via the atmosphere and the water, POPs released in one part of the world can travel to regions far from their source of origin. Under the Stockholm Convention, countries have agreed to reduce or eliminate the production, usage, and/or release of twelve key POPs known as the “dirty dozen” and that include: aldrin, chlordane, dichlorodiphenyl trichloroethane (DDT), dieldrin, endrin, heptachlor, hexachlorobenzene, mirex, toxaphene, polychlorinated biphenyls (PCBs), polychlorinated dibenzo-p-dioxins(dioxins), polychlorinated dibenzofurans (furans), PCDD/Fs. Besides these banned pollutants there are many other persistent toxic chemicals that are causing concern; amongst these also polybrominated diphenyl ethers (PBDEs) (IPEN, 2005).

PBDEs have only drawn attention as being an environmental contaminant in recent years, although they have been introduced already in the 1960's. They represent a sub-family of the brominated flame-retardants group and have been employed as flame retardants in textiles, furniture, and electronic equipment containing plastics. Especially with the emergence of personal computers and respective fire safety regulations, the environmental exposure of PBDEs has increased noticeably. Their levels have doubled just about every five years (Norén and Mieronyté, 1998). In fact, studies have shown that PBDEs have accumulated in human tissues, as evidenced by human breast milk samples from Sweden (Hooper and McDonald, 2000).

In total, there are theoretically 209 different congeners in the PBDE family which are chemically represented by $C_{12}H_{10-x}Br_xO$ (where $x = 1 \dots 10$). The numbering of the congeners is analogous to the IUPAC (International Union of Pure and Applied Chemistry) system for numbering PCBs, which is based on the position of the halogen atoms on the rings. Depending on the number of bromine atoms in the molecule, PBDEs are typically produced at

three different degrees of bromination, referred to as Penta-BDE, Octa-BDE and Deca-BDE (de Wit, 2002).

1.3 Objectives

The main objective of this study was to apply the state-of-the-art model COHERENS (Luyten et al., 1999) in order to investigate its applicability as a tool for predicting tidal flows, salinity and temperature distributions in a hypothetical estuary system. Furthermore, a contaminant module has also been included in order to analyse how the contaminant concentration of PBDE-100 is affected by the salinity and temperature distributions as well as by the exchanges with the atmosphere and sediments.

2. MODEL DESCRIPTION

In order to accurately simulate the hypothetical estuary system, the three-dimensional hydrodynamic finite-difference multi-purpose model devised for coastal and shelf seas model, called COHERENS (Luyten et al., 1999) was selected for this purpose. The COHERENS model is well-documented, freely available over the internet for research purposes and has been extensively tested. It resolves mesoscale to seasonal scale processes and consists of four principal components, namely (a) a physical part with a circulation module and a general module for solving the advection-diffusion equations, (b) an Eulerian sediment module, (c) a microplankton module and (d) a component with a Lagrangian and Eulerian contaminant transport model (Luyten et al., 1999). The source code of the program is in FORTRAN77 and is modifiable by the user to accommodate specific research objectives. Via a number of switches, the user also has the possibility to include or exclude some of the processes without the necessity of programming. For this particular application, only the hydrodynamic portion of the program along with the salinity and temperature distribution computations and contaminant module were enabled.

2.1 Hydrodynamic module

The hydrodynamic module of the COHERENS model is schematically depicted in Fig. 2.1. As can be seen, it fundamentally consists of three components of current velocity (described by equations of momentum and the continuity equation), free surface elevation dynamics, physical fields of temperature and salinity, as well as additional turbulence closure-scheme equations.

The momentum equations in COHERENS employ the Boussinesq approximation and then the pressure terms are expressed as a sum of equilibrium and perturbed parts. As a result

barotropic and baroclinic part of the pressure gradients are formulated. The barotropic part is associated with the horizontal changes of water surface and atmospheric pressure while the baroclinic one, after applying the condition for vertical hydrostatic equilibrium, represents the effect of the buoyancy. The density, used for evaluation of the buoyancy, is determined with the aid of an additional equation of state which is a function of salinity, temperature and pressure, i.e. the general equation of state of seawater defined by the Joint Panel on Oceanographic Tables and Standards (Fofonoff, 1985). Further, all vertical eddy viscosity coefficients in the momentum and scalar equations are evaluated by a turbulence closure scheme. The default turbulence scheme of COHERENS was implemented during the present simulations. This scheme defines turbulent viscosity coefficients by turbulent kinetic energy and its dissipation rate. The later quantities were found by solving an extra equation for the turbulent kinetic energy and using mixing length approximation and additional stability functions approach when describes the energy dissipation rates (Luyten et al., 1999).

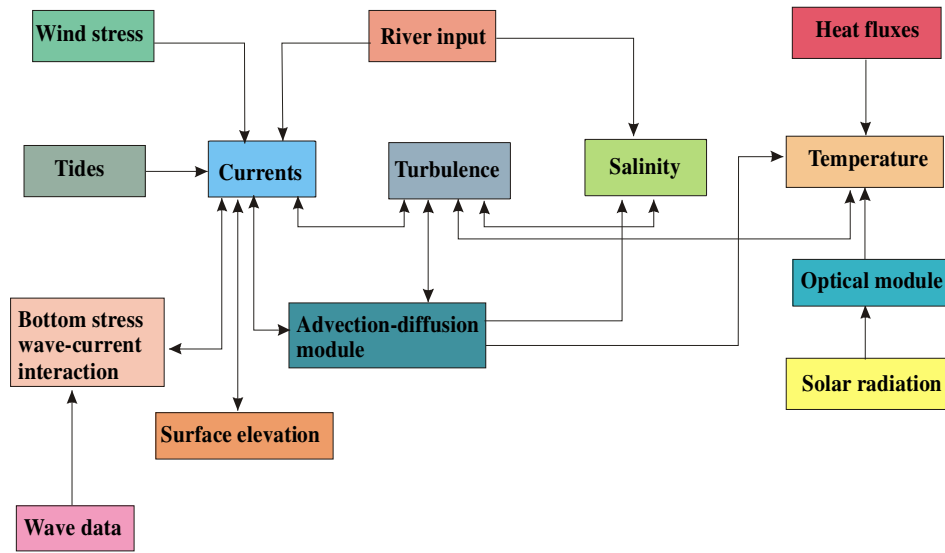


Figure 2.1 Schematic view of the hydrodynamic module of the COHERENS model.

The other governing equations in COHERENS model those about physical and turbulence fields, advection, transport, changes, fate, reactions and transformations of biogeochemical variables or dissolved and particulate fractions of contaminants in water column represent scalar transport equations of advection-diffusion type. Then the govern equation for certain scalar quantity ψ can be written mathematically in a general form as follows (Luyten *et al.*, 1999):

$$\frac{d}{dt}(\psi) = \beta(\psi), \quad \text{with} \quad \frac{d}{dt} = \mathbf{I} + \mathbf{A}_h + \mathbf{A}_v + \mathbf{A}_s - \mathbf{D}_v - \mathbf{D}_h \quad (1)$$

where t means time, ψ represents one of the model state variables, the function $\beta(\psi)$ counts for all transformations as well as source and/or sinks terms of ψ . The complex time derivative in the left side stands for transient advection-diffusion transport of ψ with: \mathbf{I} as time derivative operator, \mathbf{A}_h as horizontal advection operator, \mathbf{A}_v as vertical advection operator, \mathbf{A}_s as vertical sinking operator, \mathbf{D}_v as vertical diffusion operator and \mathbf{D}_h as horizontal diffusion operator. That is why all equations, corresponding to this general form, can be integrated numerically by “numerical solvers” implemented in the structural framework of COHERENS model. Furthermore, the solvers use mode-splitting technique (Blumberg and Mellor, 1987; Luyten et al., 1999). The method consists in solving depth-integrated momentum and continuity equations for the barotropic mode with small time steps to satisfy the stringent stability criteria for surface gravity waves, and the 3-D momentum and scalar transport equations for the baroclinic mode with a larger time steps – so called TVD (Total Variation Diminishing) scheme, an useful tool in simulations of frontal structures and areas under strong current gradients. Conservative finite differences are used to discretise the general mathematical equations in the computational space. The grid chosen for horizontal discretisation is well-known Arakawa C grid (Luyten et al., 1999) providing simple representations of both open and coastal boundaries. The commonly used sigma vertical coordinate transformation, whereby varying surface and bottom boundaries are transmitted to constant surface, is also used resulting in an equal number of elements in each vertical water column.

The numerical model domain should be specified by the solid and open boundaries, river and canal inlets and water body bathymetry. In general, the hydrodynamic and other sub-models are forced by considering: tidal and wave induced water surface changes and heat and salinity fluxes at open sea boundary, impact of river discharges and precipitation, surface shear stress and bottom friction, and surface heat fluxes depending on solar radiation, air temperature, relative humidity and cloud cover. Usually, the hydrodynamic model forcing incorporates hourly records of water surface elevation at open sea borders and daily values for the rivers’ and canals’ discharges. For horizontal currents, the surface boundary condition is formulated obtained by specifying the surface stress as a function of wind speed components, while the bottom friction is defined by slip boundary condition (Luyten et al., 1999). For the case a vertically uniform bottom shear stress is assumed yielding a logarithmic profile for the current and the bottom velocities are evaluated at grid points nearest to the bottom layer. The

quadratic bottom drag coefficient is expressed as a function of bed roughness length and uniform in space and constant in time roughness length values. Furthermore, the specific information needed to define the other model boundary conditions is extracted from hourly recorded meteorological series and daily measurements of canal discharges. Normally, the calculations start with zero initial values for currents and surface elevation and from uniform reference values for salinity, temperature and water density. No special user's efforts about different model accelerations in order to attain better convergence of the numerical solution are needed because it was found (Luyten et al., 1999) that the model itself reaches rapid and good numerical convergence.

For more detailed information about the hydrodynamic module of the COHERENS model, a full description of the COHERENS model is presented in Luyten et al. (1999).

2.2. Contaminant fate module

The affinity of organic contaminants to different environmental compartments (air, water, sediments) depends on the solubility and volatility of the compound. In fact these characteristics determine the partitioning in the dissolved and particulate-bound fraction. POPs have low water solubility and they tend to be semi-volatile, therefore, the exchange with the atmosphere plays a key role in their fate. Conversely, other organic pollutants like pesticides have in general a higher solubility and reach the surface water in the dissolved phase, carried by the rivers. Once the contaminant reaches the water body, the transport is affected by the currents and hydrodynamics. While persistent currents cause advection, currents that fluctuate over short time and space scales, like tides, result in dispersion and dilution of the contaminant.

The role of mathematical models in assessing the fate and effects of contaminants in aquatic ecosystems is continuously increasing (Koelmans *et al.* 2001). Mathematical models, once properly validated, offer the possibility to forecast the results of different plausible scenarios and to investigate the global dynamic behaviour of the studied system which would be impossible from any field experiment. However, to develop and validate such a model a considerable amount of experimental data is required.

In order to characterize the fate and transport of contaminant in the water column it is essential to accurately represent the processes occurring at the water-sediment interface as well as at the water-air interface, see Fig. 2.2, as well as the partitioning between the different phases. Besides inflow and outflow of contaminant in the system, there are several processes that affect the distribution and dynamics of contaminants, like: input from the atmosphere by wet and dry deposition, diffusive transfer of chemical across the air-water interface, settling,

resuspension, burial, diffusive exchange between the water column and sediment pore waters, bioturbation, biodiffusion and bioirrigation, and finally transformation of the compound by aerobic degradation in water and/or anaerobic degradation in the sediments.

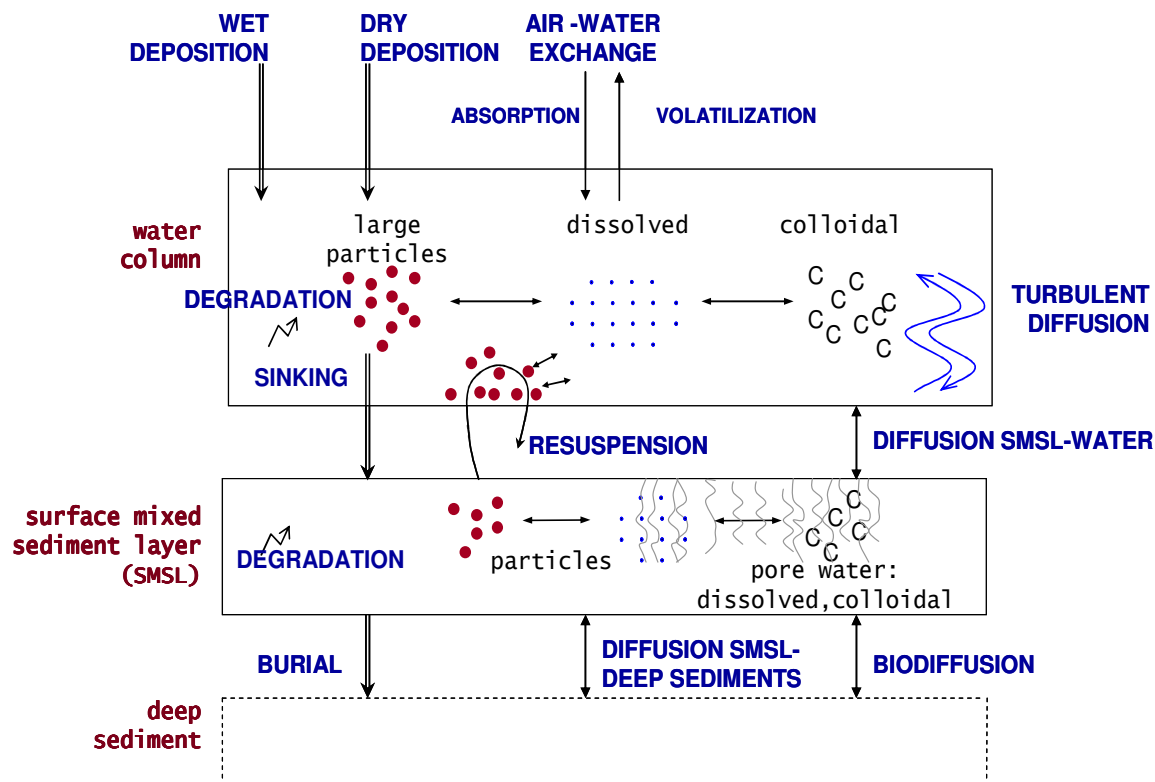


Figure 2.2 – Overview of the processes included in the contaminant fate module (Jurado et al., 2006).

For a detailed account of the equations describing the above mentioned contaminant fate and transport processes, the reader is referred to recent publications: Carafa et al. (2006), Jurado et al. (2007) and Marinov et al. (2007).

3. EXEMPLARY CASE STUDIES

For the purposes of this study, a hypothetical estuary system was constructed that consisted of a reach with a length of 26 km, with one end flowing into an estuary. To accurately characterise the hydrodynamics and salinity throughout this hypothetical estuary, the three-dimensional channel was discretised into rectangular cells with a dimension of 250m x 30m x 0.5m (length * width * depth), as shown in Fig. 3.1. Consequently, the discretised area is composed of 1664 cells. The channel is represented by the two inner grid cells

(coloured blue in Fig. 3.1) in the y-direction, while the outer grid cells in the y-direction represent a land surface (i.e., the river bank). The hydrology of this estuary system is described primarily by the tides and the freshwater influx. In order to observe the fate and transport of a typical organic contaminant, PBDE-100 has been chosen to be modelled. At the inlet the PBDE-100 contaminant is assumed to be zero but there is an initial concentration in the deep sediment layer. Therefore the contaminant will enter in the system by means of air-water and sediment-water exchanges.

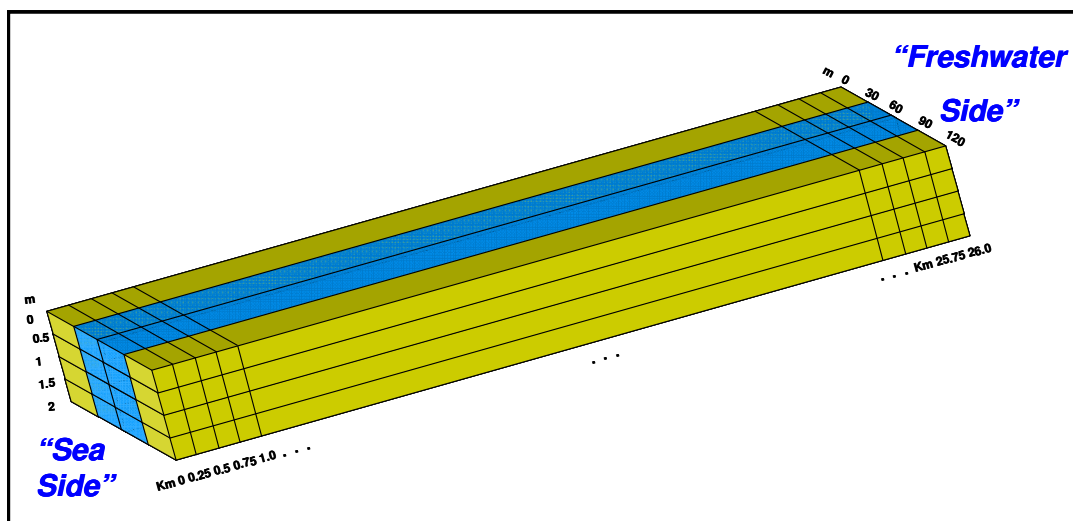


Figure 3.1 – Case study schematic

For the contaminant PBDE-100, Table 3.1 lists the specific forcing and physico-chemical parameters applied, as well as their literature references.

In order to conduct a realistic simulation of this ideal case study, actual data from the Po di Goro (Italy), a branch of the Po river estuary system for 2003 were used as input. These data included hourly meteorological data (horizontal uniform wind velocities in the x- and y-directions at 10 m height, uniform sea surface temperature, horizontal uniform relative humidity, horizontal uniform cloud coverage, horizontal uniform precipitation rate, chlorophyll *a* concentration in the sea surface measured by satellite) as well as hourly tidal amplitudes.

For investigative purposes, the model was run for two different simulation periods. The first run was 3 days (Jan. 15th – 17th 2003) and had the purpose of examining the model output according to the tidal regime (i.e., low and high tides). The first ten days of January were not considered in the run due to priming reasons of the model. During the selected three-day period the estuary experienced a semi-diurnal tide with an average range of ca. 0.9 m at the

mouth of the estuary. The tidal depths for this period are shown in Fig. 3.2. The used monitoring data identified some important characteristics relative to the temporal distribution of the tides. As can be observed, tidal peaks during this simulation period are of a bimodal character and take place daily at ca. 8:00-9:00 and 22:00-23.00 hours, while tidal lows occur unimodally and daily around 16:00-17.00 hours.

Table 3.1 – Typical PBDE-100 ranges and corresponding references

Parameter	Range	Refer.
Gaseous concentration in the atmosphere [ng m ⁻³]	Typical PBDE range: 0.49-73.00 ng m ⁻³ (Lake Maggiore, Italy) PBDE-100: 1.30E-03	Mariani et al, 2006
Particulate concentration in the atmosphere [ng m ⁻³]	Typical PBDE range: 1.69-17.22 10 ⁻³ ng m ⁻³ (Lake Maggiore, Italy) PBDE-100: 4.19E-03	Mariani et al, 2006
Rain concentration (dissolved + particulate) [ng m ⁻³]	Typical PBDE range: 35-630 ng m ⁻³ (Lake Maggiore, Italy) PBDE-100: 140	Mariani et al, 2006
Total concentration in the deep sediments [ng m ⁻³]	Typical PBDE range: 1.8810 ⁺⁵ -1.8410 ⁺⁷ ng m ⁻³ (Lake Maggiore, Italy) PBDE-100: 1.88E+05	Mariani et al, 2006
Molecular weight [g/mol]	PBDE-100: 564.6874	Mariani et al, 2006
Molar volume [cm ³ /mol]	PBDE-100: 311.0	
Dimensionless Henry values varing with temperature according to $\ln H^* = A_h - B_h / T$	PBDE-100: A_h 12.7 B_h 6515	Cetin and Odabasi (2005)
Octanol water partition coefficient at 298K used after for $K_{OW} = K_{OW_{298}} \exp(\Delta H_s / R * (1/T_w - 1/298))$	PBDE-100: 1.123E+7	Tomy et al., 2001, Tittlemier et al., 2002, Breakvelt et al., 2003, Ellinger et al, 2003; Wania and Dugani, 2003
Partition coefficient of the chemical between organic carbon and water [m ³ ng ⁻¹]	$\log K_{OC} = A_{OC} \log K_{OW} + B_{OC}$ $A_{OC} = 0.81$ $B_{OC} = 0.1$	EU 2002
Partition coefficient of the chemical between octanol and air (temperature dependant) [m ³ ng ⁻¹]	$\log K_{OA} = A_{OA} + B_{OA} / T$ A_{OA} B_{OA} PBDE-100: -7.18 5459	Harner (2001), and Wania & Dugani (2003) for BDE209
Degradation rate [1/s]	PBDE-100: Water: 5.34836E-8 Sediment: 1.333709E-8	(Palm et al. 2002)

The theoretically measured air temperature and salinity distributions for the open sea and river ends for the three-day period are depicted in Fig. 3.3. The air temperatures at the open sea and river ends are quite constant, with the open sea end having slightly higher air temperatures. The salinity distributions for each end, on the other hand, show that the salinities at the freshwater end are appreciably lower. It should be noted, however, that for the entire simulation period a constant river end salinity of 3.0 PSU was assumed and implemented in the model.

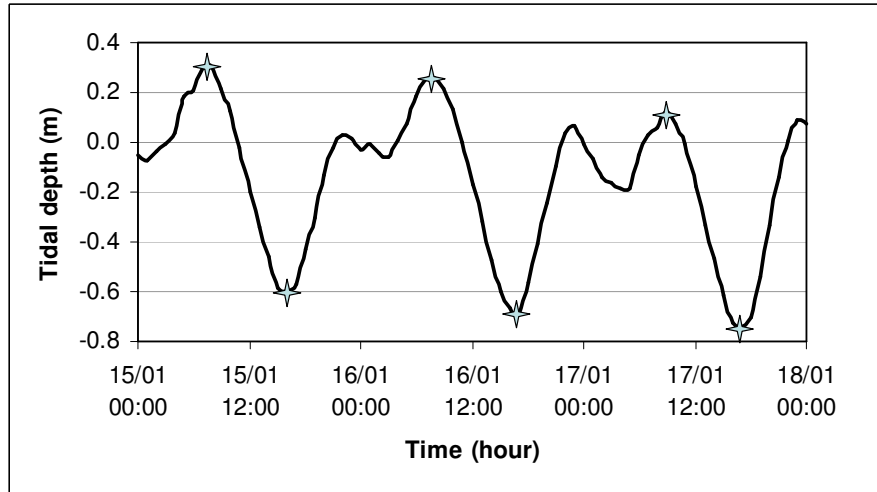


Figure 3.2. Tidal depth for the period 15/01/2003 – 17/01/2003

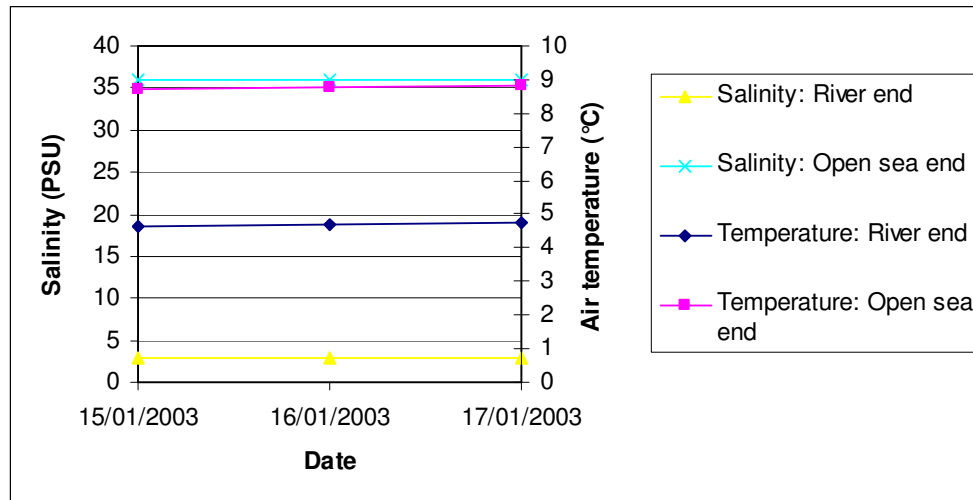


Figure 3.3. Theoretically measured temperature and salinity distribution at the open sea and river ends for the simulation period

The second investigative model run, on the other hand, embodied a simulation period of 1 year (year 2003). This run was undertaken to observe if the model's behaviour with regard to temperature, salinity and PBDE-100 concentration could be justified and deemed reasonable.

4. RESULTS AND DISCUSSION

4.1. 3-Day Simulation

Figures 4.1 to 4.6 show the temperature, salinity and contaminant distributions, respectively, for six points in time (these points are indicated by crosses in Figure 3.2). These six temporal points have been selected to observe changes as well as synergy with respect to temperature, salinity and PBDE-100 contaminant concentration during low and high tidal periods.

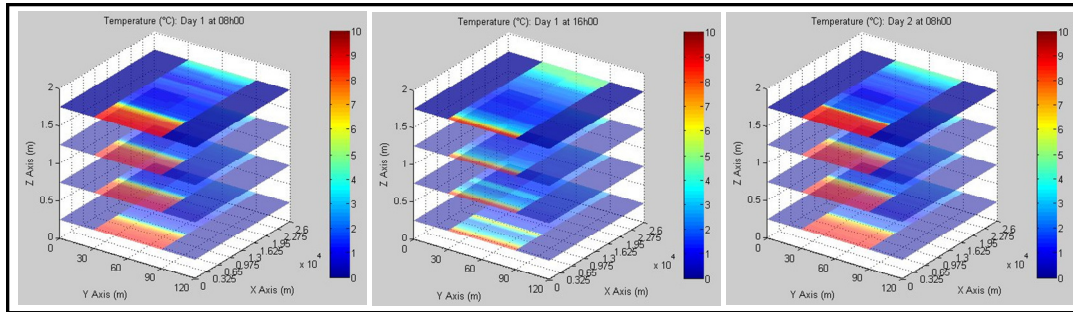


Figure 4.1: Temperature distribution for Day 1 at 08h00, Day 1 at 16h00 and Day 2 at 08h00

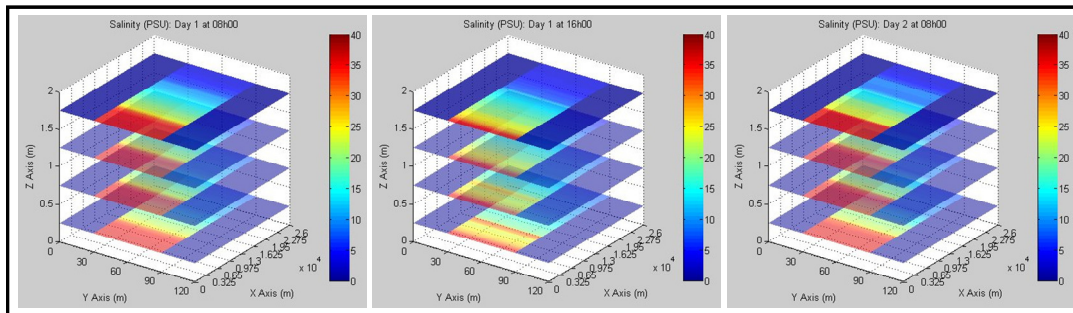


Figure 4.2: Salinity distribution Day 1 at 08h00, Day 1 at 16h00 and Day 2 at 08h00

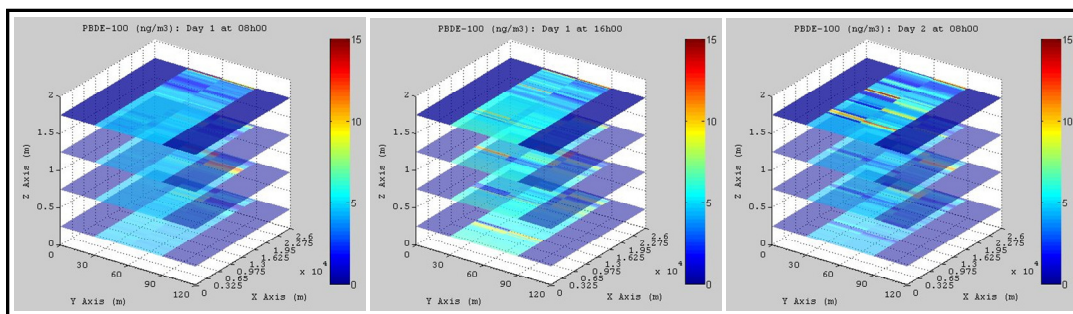


Figure 4.3: PBDE-100 distribution Day 1 at 08h00, Day 1 at 16h00 and Day 2 at 08h00

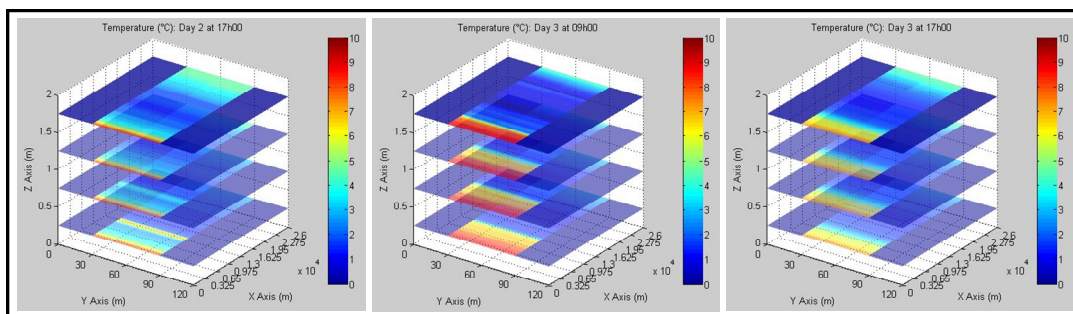


Figure 4.4: Temperature distribution for Day 2 at 17h00, Day 2 at 09h00 and Day 3 at 17h00

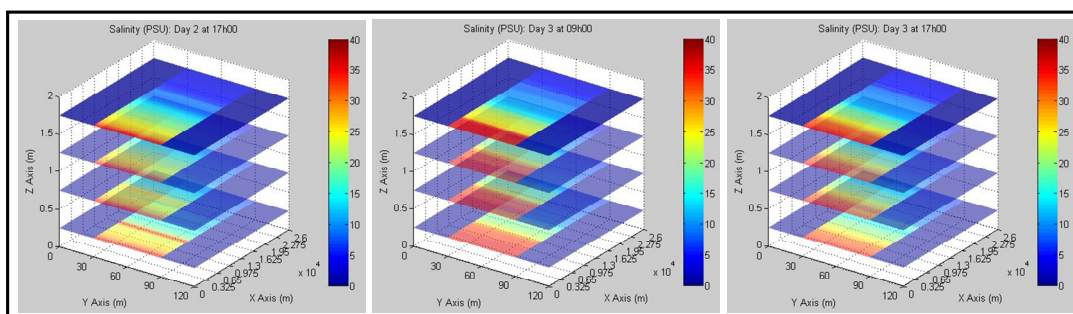


Figure 4.5: Salinity distribution for Day 2 at 17h00, Day 2 at 09h00 and Day 3 at 17h00

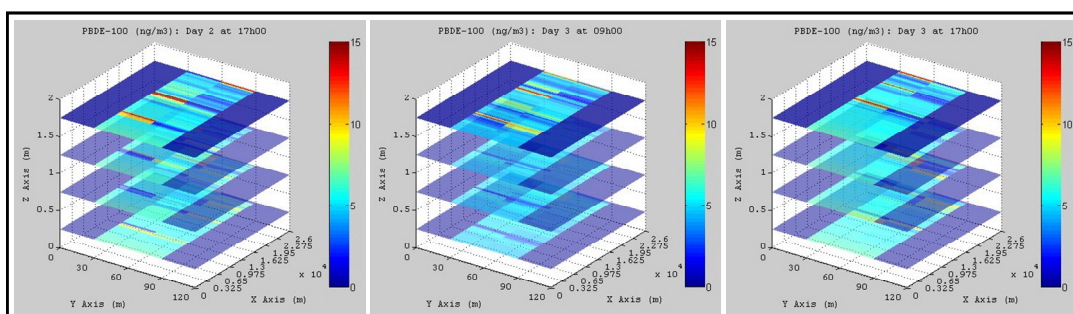


Figure 4.6: PBDE-100 distribution for Day 2 at 17h00, Day 2 at 09h00 and Day 3 at 17h00

From Figures 4.1 to 4.6, one can see that the spatial temperature distributions within the channel largely reflect a conservative mixing of heat contents between the sea water and fluvial water. Salinity reflects the tidal dynamics and PBDE-100 concentration shows the dilution effects of sea water considered not contaminated.

In addition, three points within the centre of the channel were chosen (at the sea side, centre channel and river side) to graphically investigate the course of the temperature, salinity and contaminant concentration within this 3-day period. Figure 4.7 gives a pictorial overview of the locations of these chosen three points. Figures 4.8 to 4.10, on the other hand, depict the temperature, salinity and PBDE-100 concentration during this 3-day period.

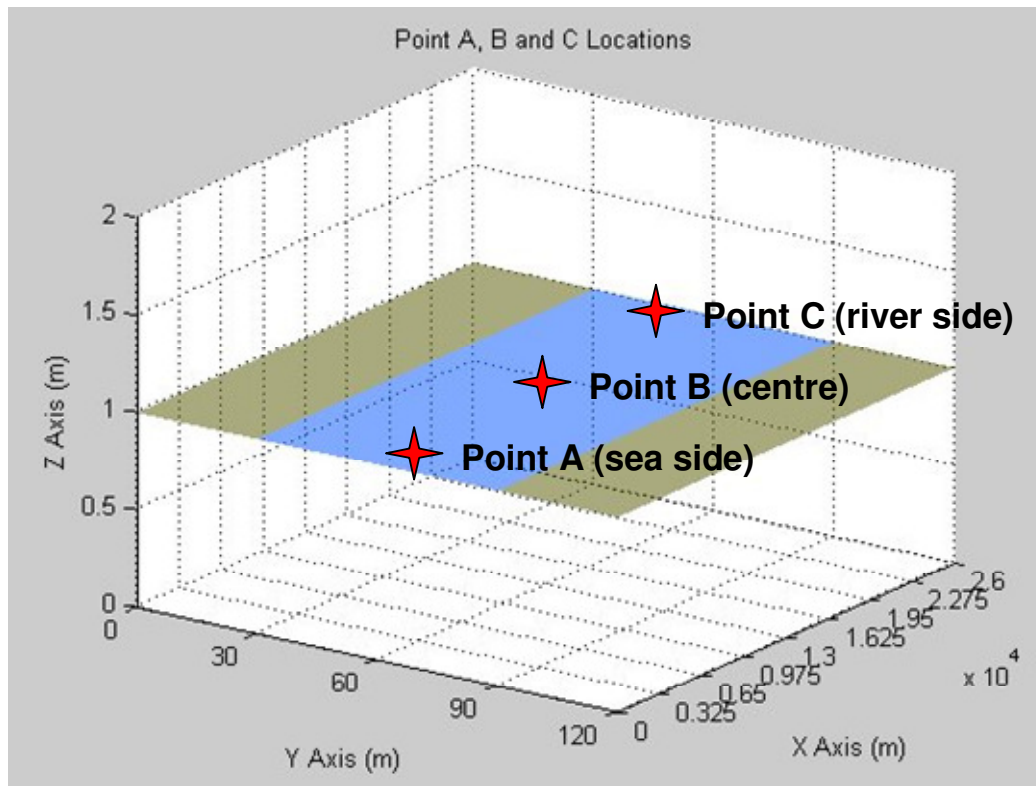


Figure 4.7 – Point locations of observed temporal evolutions

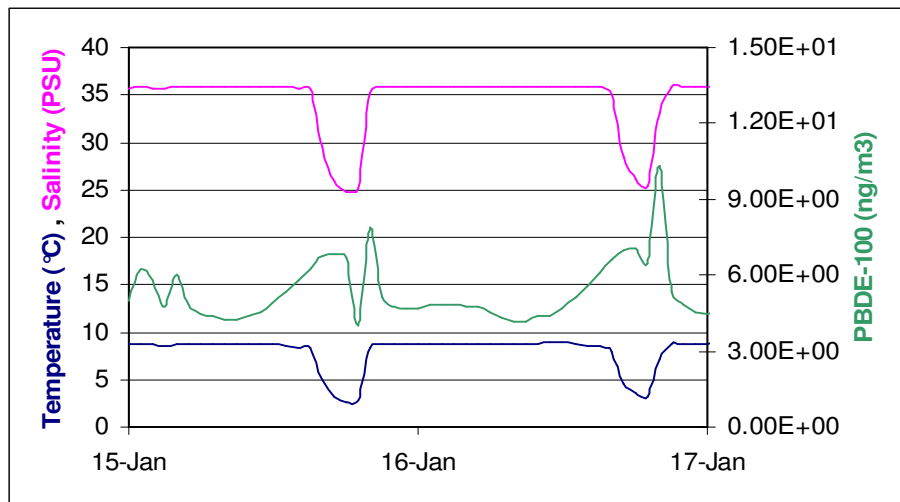


Figure 4.8. Temperature, Salinity and PBDE-100 concentration during the 3-day simulation period (Point A: sea side).

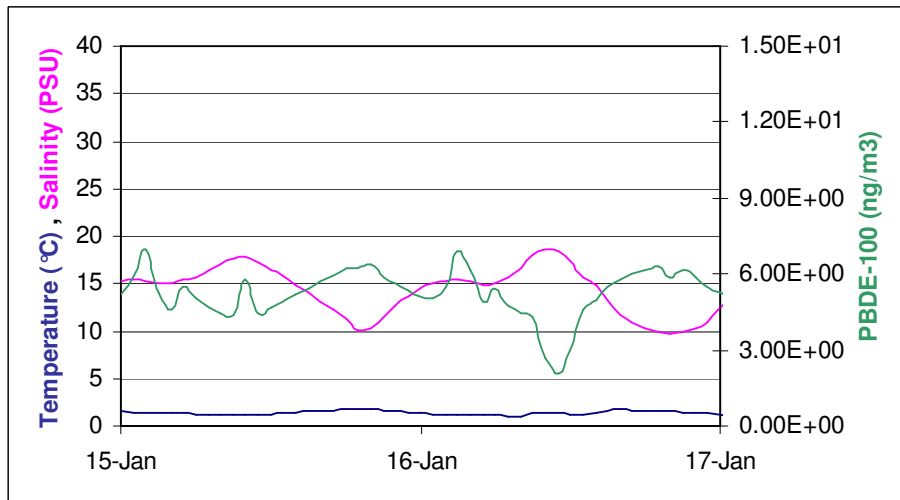


Figure 4.9. Temperature, Salinity and PBDE-100 concentration during the 3-day simulation period (Point B: centre channel).

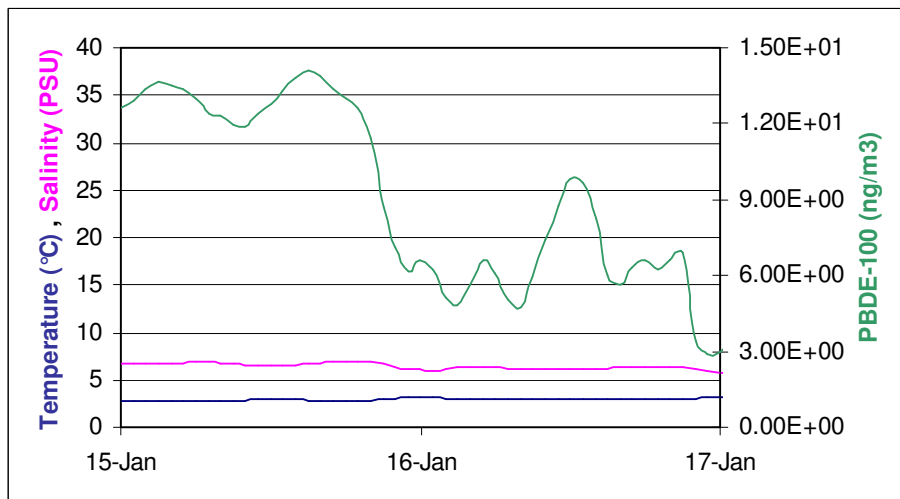


Figure 4.10. Temperature, Salinity and PBDE-100 concentration during the 3-day simulation period (Point C: river side).

From a closer look at the above figures, the following observations can be made. On the sea side, the temperature and salinity increase with higher tides, and advance towards the river side. Simultaneously, the contaminant PBDE-100 decreases with increasing tide on the sea side. On the river side, on the other hand, the opposite occurs: temperature and salinity slightly decrease with higher tides.

From Fig. 4.8, it can be seen that at the sea side as temperature and salinity drop at certain times of the day, the PBDE-100 concentration increases sharply at those points in time. The temperature at the river side, on the other hand, remains approximately constant during the 3-day simulation period.

4. 2. 1-Year Simulation

With regard to the 1-year simulation, the same three points within the centre of the channel were chosen (at the sea side, centre channel and river side) and used to investigate the temporal evolution of the temperature, salinity and contaminant concentration. The time step used for the model output was one hour.

Figures 4.11 to 4.13 show the temporal evolution of temperature, salinity, and PBDE-100 concentration at the sea side, centre channel and river side, respectively. Due to priming issues of the model, the first ten days in January are not shown in Figures 4.11 to 4.13.

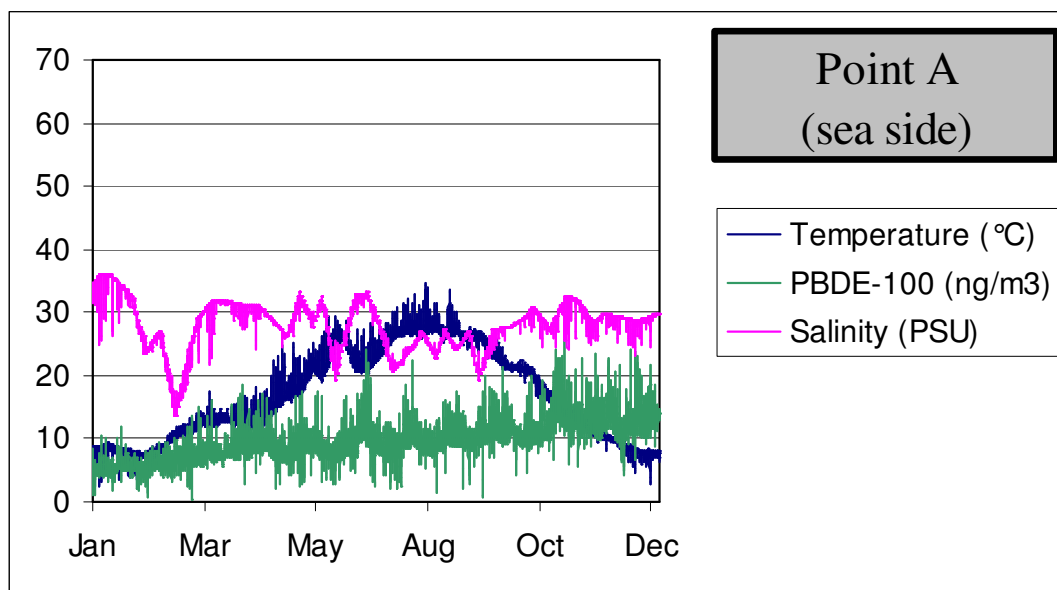


Figure 4.11 – Temperature, salinity and PBDE-100 concentration at sea side (2003)

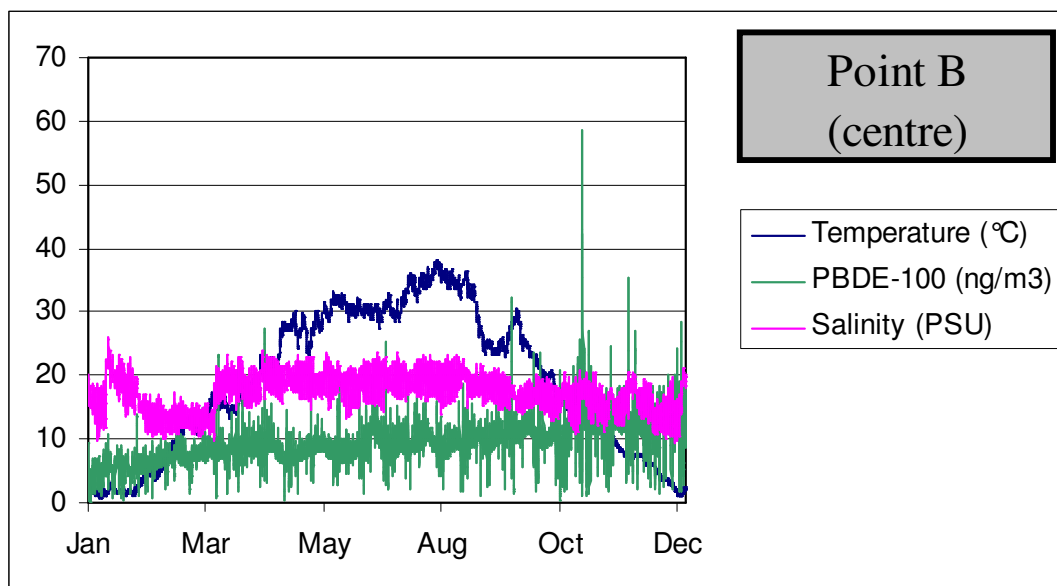


Figure 4.12 – Temperature, salinity and PBDE-100 concentration at centre channel (2003)

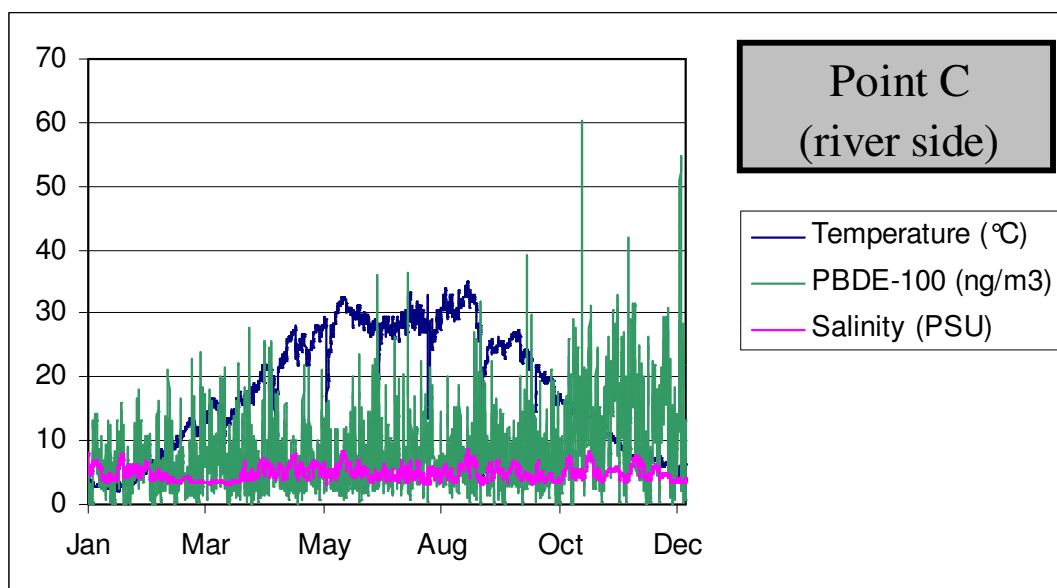


Figure 4.13 – Temperature, salinity and PBDE-100 concentration at river side (2003)

The following observations can be made from Figures 4.11 to 4.13. At all three point locations a steady increase in PBDE-100 concentration over the 1-year time period can be witnessed. This is probably due to the concentration values in the deep sediment whereas the oscillations are probably due to the fact that sediment-water exchange depends on the flow velocities. Peak values are normally due to wet deposition during rain events. The temperature distribution for the year can be classified as normal, with highs in the summer

months and lower temperatures during the winter period. The temperature profiles accurately reflect the seasonality in the estuary. In this hypothetical estuary system, the temperature of freshwater is generally higher than that of coastal waters during autumn and late winter (October-February). However, this trend is reversed by August, when the highest temperatures are recorded on the sea side. Therefore, variations in temperature may influence interactions between physical and chemical processes in this estuary. During periods of high precipitation, the estuary system experiences a maximal freshwater input which leads to the displacement of the freshwater-saltwater interface down the estuary. The net freshwater flow originating from the river side does not contribute significantly to the hydrodynamic conditions. Nonetheless, it usually controls many of the water quality variables, including the salinity and temperature distributions along the estuary. The turbulent mixing and dispersion phenomena are controlled by the local tidal velocity conditions in the estuary, which in turn, affect the temperature and salinity distributions along the estuary. The salinity distribution at the river end primarily depends on the freshwater flow conditions and secondarily on the tidal flow conditions in the estuary. The salinity conditions at the sea side end exceed 35 PSU at the end of January. The salinity decreases rapidly along the upstream direction toward the river end.

5. CONCLUSIONS

The proposition underlying this research effort has been a basic one: COHERENS model can be applied to realistically simulate tidal flows, salinity and temperature distributions, as well as PBDE-100 contaminant fate and transport in estuaries. Given the input data and model parameters used for the simulations, the following conclusions can be made about COHERENS' feasibility for the objectives set. Within the realm of the performed simulations, COHERENS appears to be suitable for the research undertaken here. However, as the geometry of the estuary is ideal and some of the model input and forcing parameters have only been roughly estimated, it would be highly recommendable to fine-tune these to more realistic values.

Concerning the contaminant module, even though it has produced reliable results for other chemical families (Carafa et al., 2006; Zaldivar et al., 2007) the validation for PBDEs is still pending due to the unavailability of experimental data. In addition a more careful study on the role of salinity on sediment-water exchange would be necessary.

Finally, in order to validate this model, field studies collecting data for a specific estuary should be undertaken. Data collection should focus on air and sediment concentrations which

will provide the forcing for the model as well as water concentrations which will serve to validate the results.

6. REFERENCES

- Batiuk, R., Bergstrom, P., Kemp, M., Koch, E., Murray, L., Stevenson, C., Bartleson, R., Carter, V., Rybicki, N., Landwehr, J., Gallegos, C., Karrh, L., Naylor, M., Wilcox, D., Moore, K., Ailstock, S. and Teichberg, M. 2000. Chesapeake Bay submerged aquatic vegetation water quality and habitat-based requirements and restoration targets: A second technical synthesis. CBP/TRS 245/00. EPA 903-R-00-014, U.S. EPA, Chesapeake Bay Program, Annapolis, MD.
- Blumberg, A.F. and Mellor, G.L. 1987. A description of a three-dimensional coastal ocean circulation model. In: N.S. Heaps, Editor, Three-dimensional Coastal Ocean Models. Coastal and Estuarine Sciences vol. 4, American Geophysical Union, Washington D.C., pp. 1–16.
- Carafa, R., Marinov, D., Dueri, S., Wollgast, J., Ligthart, J., Canuti, E., Viaroli, P. and Zaldívar, J. M., 2006. A 3D hydrodynamic fate and transport model for herbicides in Sacca di Goro coastal lagoon (Northern Adriatic). *Marine Pollution Bulletin* **52**:1231-1248.
- Chatwin, P.C. 1976. Some remarks on the maintenance of the salinity distribution in estuaries. *Estuarine and Coastal Marine Science* **4**:555-566.
- De Wit, C.A. 2002. An overview of brominated flame retardants in the environment. *Chemosphere* **46**:583-624.
- Fofonoff, N.P. 1985. Physical properties of seawater: a new salinity scale and equation of state for seawater, *Journal of Geophysical Research* **90**(C2):3332–3343.
- Garrison, T. 1995. Essentials of Oceanography. Wadsworth Publishing Company, Belmont, CA. 353 pp.
- Greger, M., Kautsky, L. and Sandberg, T. 1995. A tentative model of Cd uptake in *Potamogeton pectinatus* in relation to salinity. *Environmental and Experimental Botany* **35**:215-225.
- Hansen, D.V. and Rattray, M. 1965. Gravitational Circulation in Straits and Estuaries. *Journal of Marine Research* **23**:104-122.
- Hetland, R.D. and Geyer, W.R. 2004. An idealized study of the structure of long, partially mixed estuaries. *Journal of Physical Oceanography* **34**:2677-2691.
- Hooper, K. and McDonald, T.A. 2000. The PBDEs: An emerging environmental challenge and another reason for breast-milk monitoring programs. *Environmental Health Perspectives* **108**(5):387-392.
- IPEN. 2005. International POPs Elimination Network. Body Burden Community Monitoring Handbook. Last Accessed Dec. 17, 2007. Available at: <http://www.oztoxics.org/cmwg/>.
- Jackson, P.R. and Rehmann, C.R. 2003. Kinematic Effects of Differential Transport on Mixing Efficiency in a Diffusively Stable, Turbulent Flow. *Journal of Physical Oceanography* **33**:299-304.
- Jurado, E., Zaldivar, J.M., Marinov, D. and Dachs, J. 2007. Fate of persistent organic pollutants in the water column: Does turbulent mixing matter? *Marine Pollution Bulletin* **54**: 441-451.
- Kautsky, L. 1998. Monitoring eutrophication and pollution in estuarine environments: Focusing on the use of benthic communities. *Pure & Applied Chemistry* **70**:2313-2318.
- Koelmans, A. A., Van der Heijde, A., Knijff, L. M. and Alderink, R.H. 2001. Integrated modelling of eutrophication and organic contaminant fate and effects in aquatic ecosystems. A review. *Water Research* **35**:3517-3536.
- Kranenburg, C. 1986. A time scale for long-term salt intrusion in well-mixed estuaries. *Journal of Physical Oceanography* **16**:1329-1331.

-
- Li, M., Zhong, L. and Boicourt, W.C. 2005. Simulations of Chesapeake Bay estuary: Sensitivity to turbulence mixing parameterizations and comparison with observations, *Journal of Geophysical Research* **110**:C12004.
- Liu, W.C., Hsu, M.H. and Kuo, A.Y. 2002. Application of different turbulence closure model for stratified tidal flows and salinity in an estuarine system. *Mathematics and Computers in Simulation* **59**:437-451.
- Luyten, P.J., Jones, J.E., Proctor, R., Tabor, A., Tett, P. and Wild-Allen, K. 1999. COHERENS—a coupled Hydrodynamical–Ecological Model for Regional and Shelf Seas: User Documentation. MUMM Report. Management Unit of the Mathematical Models of the North Sea, 911 pp.
- MacCready, P. 1999. Estuarine adjustment to changes in river flow and tidal mixing. *Journal of Physical Oceanography* **29**:708-726.
- Marinov, D., Dueri, S., Puillat, I., Zaldívar, J.-M., Jurado, E. And Dachs, J. 2007. Description of contaminant fate model structure, functions, input data, forcing functions and physico-chemical properties data for selected contaminants (PCBS, PBDEs, PCDD/Fs). Institute for Environment and Sustainability. Joint Research Centre. EUR 22627. 71 pp.
- Monismith, S.G. and Fong, D.A. 1996. A simple model of vertical mixing in a stratified tidal flow. *Journal of Geophysical Research* **101**:28583-28595.
- Norén, K and Mieronyté, D. 1998. Contaminants in Swedish human milk: Decreasing levels of organochlorine and increasing levels of organobromine compounds. *Organohalogen Compounds* **35**:1–4.
- North, E.W., Chao, S.Y., Sanford, L.P. and Hood, R.R. 2004. The influence of wind and river pulses on an estuarine turbidity maximum: numerical studies and field observations in Chesapeake Bay. *Estuaries* **27**:132-146.
- Nunes Vaz, R.A., Lenon, G.W. and de Silva Samarasinghe, J.R. 1989. The negative role of turbulence in estuarine mass transport. *Estuarine, Coastal, and Shelf Science* **28**:361-377.
- Nunes Vaz, R.A. and Simpson, J.H. 1994. Turbulence closure modelling of estuarine stratification. *Journal of Geophysical Research* **99**:16143-16160.
- OSPAR. 2000. Quality Status Report 2000. Monitoring and Assessment Series. n.111. pp108.
- Prandle, D. 2004. Saline intrusion in partially mixed estuaries. *Estuarine, Coastal and Shelf Science* **59**:385-397.
- Simpson, J.H., Brown, J., Matthews, J. and Allen, G. 1990. Tidal straining, density currents, and stirring in the control of estuarine stratification. *Estuaries* **13**:125-132.
- Simpson, J.H. and Sharples, J. 1991. Dynamically-active models in the prediction of estuarine stratification, in *Dynamics and Exchanges in Estuaries and the Coastal Zone*, D. Prandle (ed.), Springer-Verlag, New York, 101-113.
- Simpson, J.H., Sharples, J. and Rippeth, T.P. 1991. A prescriptive model of stratification induced by freshwater runoff. *Estuarine, Coastal, and Shelf Science* **33**:23-35.
- Stenstrom, P. 2004. Hydraulics and mixing in the Hudson River Estuary: A numerical model study of the tidal variations during neap tide conditions. *Journal of Geophysical Research* **109**:C04019.
- Turner, A. and Rawling M. C. 2001. The influence of salting out on the sorption of neutral organic compounds in estuaries. *Wat. Res.* **35**, 4379-4389.
- Turner, A. 2003. Salting out of chemical in estuaries: implications for contaminant partitioning and modelling. *The Science of Total Environment* 314-316, 599-612.
- UNEP. 2004. Integrated Watershed Management - Ecohydrology and Phytotechnology Manual. UNESCO, United Nations Environment Programme. 246 pp.
- U.S. EPA. 2006. Volunteer Estuary Monitoring: A Methods Manual. Publication EPA-842-B-06-003.
- Warner, J.C., Geyer, W.R. and Lerczak, J.A. 2005. Numerical modelling of an estuary: A comprehensive skill assessment, *Journal of Geophysical Research* **110**:C05001.

-
- Wei, H., Wu, J. and Zhang, P. 2001. Review of turbulence closure models in ocean hydrodynamics. *Journal of Ocean University Qingdao* **31**:7-13.
- Wunsch, C. and Ferrari, R. 2004. Vertical mixing, energy, and the general circulation of the oceans. *Annual Review of Fluid Mechanics* **36**:281-314
- Zhou, M. 1998. Influence of bottom stress on the two-layer flow induced by gravity currents in estuaries. *Estuarine, Coastal, and Shelf Science* **46**:811-825.
- Zaldívar, J.M., Marinov, D., Dueri, S., Puillat, I., Carafa, R., Berrojalbiz, N., Lacorte, S., Jurado, E. and Dachs, J. 2007. Integrated Modeling of Fate and Effects of Persistent Organic Pollutants in Marine Ecosystems. EUR 22882 EN. 47 pp.

EUR 23227 EN – Joint Research Centre

Title: **PBDE contaminant fate transport in an estuary using a three-dimensional hydrodynamic modelling**

Author(s): R.O. Strobl, I. Puillat, D. Marinov, S. Dueri and J. M. Zaldívar

Luxembourg: Office for Official Publications of the European Communities

2007 – 29 pp. – 21 x 29,7 cm

EUR – Scientific and Technical Research series – ISSN 1018-5593

Abstract.

The fate and transport of contaminants in estuaries is still not completely understood due to the extremely high physico-chemical variability in these environments. In this report, a 3D hydrodynamic model has been applied for estuary modelling to predict tidal flows, salinity and temperature distributions; and for the fate and transport of Polybrominated Diphenyl Ethers (PBDEs). With this goal in mind, a hypothetical estuary system was constructed that consisted of a reach with a length of 26 km. Consequently, the hydrology of this estuary system was described primarily by the tides and the freshwater influx. The contaminant PBDE-100 was assumed to enter by means of river transport, exchange with sediments and atmospheric inputs. Two simulations were undertaken, namely one of three days and the other of one year, in order to observe how and if the model realistically had simulated the fate transport of PBDE-100 in the hypothetical estuary system. The simulations performed have shown that the model is able to represent adequately the hydrodynamic aspects as well as the typical temperature and salinity distributions. Concerning the contaminant distribution the model shows the importance of atmospheric processes as well as the role of sediments as, in this case, a source of contaminant. The next step will consist on applying this model to a real estuary and validate it with experimental data.

The mission of the JRC is to provide customer-driven scientific and technical support for the conception, development, implementation and monitoring of EU policies. As a service of the European Commission, the JRC functions as a reference centre of science and technology for the Union. Close to the policy-making process, it serves the common interest of the Member States, while being independent of special interests, whether private or national.

